



Grid Gap Measurement for an NSTAR Ion Thruster

Esther M. Diaz and George C. Soulas
Glenn Research Center, Cleveland, Ohio

NASA STI Program . . . in Profile

Since its founding, NASA has been dedicated to the advancement of aeronautics and space science. The NASA Scientific and Technical Information (STI) program plays a key part in helping NASA maintain this important role.

The NASA STI Program operates under the auspices of the Agency Chief Information Officer. It collects, organizes, provides for archiving, and disseminates NASA's STI. The NASA STI program provides access to the NASA Aeronautics and Space Database and its public interface, the NASA Technical Reports Server, thus providing one of the largest collections of aeronautical and space science STI in the world. Results are published in both non-NASA channels and by NASA in the NASA STI Report Series, which includes the following report types:

- **TECHNICAL PUBLICATION.** Reports of completed research or a major significant phase of research that present the results of NASA programs and include extensive data or theoretical analysis. Includes compilations of significant scientific and technical data and information deemed to be of continuing reference value. NASA counterpart of peer-reviewed formal professional papers but has less stringent limitations on manuscript length and extent of graphic presentations.
- **TECHNICAL MEMORANDUM.** Scientific and technical findings that are preliminary or of specialized interest, e.g., quick release reports, working papers, and bibliographies that contain minimal annotation. Does not contain extensive analysis.
- **CONTRACTOR REPORT.** Scientific and technical findings by NASA-sponsored contractors and grantees.

- **CONFERENCE PUBLICATION.** Collected papers from scientific and technical conferences, symposia, seminars, or other meetings sponsored or cosponsored by NASA.
- **SPECIAL PUBLICATION.** Scientific, technical, or historical information from NASA programs, projects, and missions, often concerned with subjects having substantial public interest.
- **TECHNICAL TRANSLATION.** English-language translations of foreign scientific and technical material pertinent to NASA's mission.

Specialized services also include creating custom thesauri, building customized databases, organizing and publishing research results.

For more information about the NASA STI program, see the following:

- Access the NASA STI program home page at <http://www.sti.nasa.gov>
- E-mail your question via the Internet to help@sti.nasa.gov
- Fax your question to the NASA STI Help Desk at 301-621-0134
- Telephone the NASA STI Help Desk at 301-621-0390
- Write to:
NASA STI Help Desk
NASA Center for AeroSpace Information
7121 Standard Drive
Hanover, MD 21076-1320



Grid Gap Measurement for an NSTAR Ion Thruster

Esther M. Diaz and George C. Soulas
Glenn Research Center, Cleveland, Ohio

Prepared for the
29th International Electric Propulsion Conference
cosponsored by ERPS, Princeton University, NASA Glenn, NASA Jet Propulsion Laboratory, Aerojet,
EPPDYL, IEPC, Busek Company, Inc., and Mitsubishi Electric
Princeton, New Jersey, October 31–November 4, 2005

National Aeronautics and
Space Administration

Glenn Research Center
Cleveland, Ohio 44135

This report contains preliminary findings,
subject to revision as analysis proceeds.

Level of Review: This material has been technically reviewed by technical management.

Available from

NASA Center for Aerospace Information
7121 Standard Drive
Hanover, MD 21076-1320

National Technical Information Service
5285 Port Royal Road
Springfield, VA 22161

Available electronically at <http://gltrs.grc.nasa.gov>

Grid Gap Measurement for an NSTAR Ion Thruster

Esther M. Diaz and George C. Soulas
National Aeronautics and Space Administration
Glenn Research Center
Cleveland, Ohio 44135

The change in gap between the screen and accelerator grids of an engineering model NSTAR ion optics assembly was measured during thruster operation with beam extraction. The molybdenum ion optics assembly was mounted onto an engineering model NSTAR ion thruster. The measurement technique consisted of measuring the difference in height of an alumina pin relative to the downstream accelerator grid surface. The alumina pin was mechanically attached to the center aperture of the screen grid and protruded through the center aperture of the accelerator grid. The change in pin height was monitored using a long distance microscope coupled to a digital imaging system. Transient and steady-state hot grid gaps were measured at three power levels: 0.5, 1.5 and 2.3 kW. Also, the change in grid gap was measured during the transition between power levels, and during the startup with high voltage applied just prior to discharge ignition. Performance measurements, such as perveance, electron backstreaming limit and screen grid ion transparency, were also made to confirm that this ion optics assembly performed similarly to past testing. Results are compared to a prior test of 30 cm titanium ion optics.

I. Introduction

The NSTAR (i.e. NASA Solar Electric Propulsion Technology Applications Readiness program) ion thruster system on the Deep Space 1 mission demonstrated the viability of ion propulsion for deep space missions.¹ As a result, the NSTAR ion propulsion system will be used as the primary propulsion system for the Dawn mission,² and continues to be a candidate for deep space missions, such as NASA Discovery-class missions.

A critical NSTAR thruster dimension that affects thruster performance and service life is the gap between the screen and accelerator grids of the ion optics assembly. While this grid gap is preset during ion optics assembly (i.e. cold grid gap), the grid gap during engine operation (i.e. hot grid gap) changes due to differential heating and, therefore, thermal expansion of the screen and accelerator grids. Knowledge of this hot grid gap is essential in properly assessing ion optics' performance parameters and service life.

A prior study demonstrated a new technique for measuring the hot grid gap during ion engine operation with and without beam extraction.³ This technique consisted of an alumina pin that was mechanically attached to the center aperture of the screen grid and passed through the center aperture of the accelerator grid. To obtain the measurement of the gap between the grids, the tip of the alumina pin and the downstream section of the accelerator grid were used as the references points. A system composed of a long distance microscope attached to a CCD camera imaged the pin during thruster operation. The ion optics and the alumina pin were illuminated using two halogen bulbs.

This technique was successfully used to measure the hot grid gap of a 30 cm titanium ion optics assembly.³ This study yielded several findings. First, the hot grid gaps with and without beam extraction were found to be different due to changes in power deposition to the grids from the plasma. As a result, hot grid gap measurements without beam extraction, such as those of Ref. 4, are not necessarily the same as those with beam extraction. Second, the hot grid gap can vary at different thruster power levels. Finally, the hot grid gap was found to be significantly smaller

than the cold grid gap. At full power, for example, the hot grid gap at the ion optics' center was about half that of the cold grid gap.

The latter finding lent insight into the hot grid gap of the NSTAR molybdenum ion optics. This is because this titanium ion optics assembly, which is nearly identical in design to the NSTAR molybdenum ion optics, performed similarly to the NSTAR optics.^{5,6} Thus, the hot grid gaps of the ion optics were likely similar. More importantly, however, the hot grid gaps of the NSTAR ion optics were likely considerably smaller than anticipated based on the past measurements from Ref. 4.

The objective of this study was to measure the change in hot grid gap of a NSTAR molybdenum ion optics assembly. Transient and steady-state hot grid gaps were measured at three power levels: 0.5, 1.5 and 2.3 kW. Also, the change in grid gap was measured during the transition between power levels, and during the startup with high voltage applied just prior to discharge ignition. Performance measurements, such as perveance, electron backstreaming limit and screen grid ion transparency, were also made to confirm that this ion optics assembly performed similarly to past testing. Results were compared to those of the 30 cm diameter titanium ion optics.

II. The Hot Grid Gap Measurement Technique

The hot grid gap measurement technique, described in Ref. 3, consisted of measuring the relative height of an alumina pin during thruster operation. The alumina pin was cemented onto a small base that was mechanically attached to the screen grid, as shown in Fig 1. The pin was located at the geometric center of the perforated region of the grid electrode. Only four screen grid apertures were covered by the pin assembly. The alumina pin passed through the center aperture of the accelerator grid and was centered within it to avoid contact with the accelerator grid. The insulator material of the pin allowed thruster operation with minimal disturbance, so that hot grid gap measurements with beam extraction could be made. The largest change in measured grid gap was limited by the screws that mounted the pin to the screen grid. The largest change in grid gap was -0.43 mm.

An imaging system monitored the pin assembly during testing. This system is to the same as that used in Ref 3, which consisted of a long distance microscope attached to a CCD camera and coupled to a computer. The camera was mounted onto a two-axis positioning system that aided in focusing on the alumina pin. The camera was also located about 0.5 m away from the thruster to preclude direct beam ion impingement which could damage the camera and lens during thruster operation with beam extraction.

A sample of the resulting image is shown in Fig 2. On this figure, the reference points used to measure the pin height giving the change in grid gap are indicated. Reference point 1 is the alumina pin tip, which gives the screen grid reference position. Reference point 2 is a point on the downstream surface of the accelerator grid. The change in grid gap was obtained by measuring the change in distance between the two reference points. Grid movement was determined measuring the change in distance of each reference point relative to its initial position just prior to thruster operation. All measurements were calibrated with the pin diameter, which was measured prior to testing. It is important to clarify that the grid movement presented in this study does not include overall movement of the thruster; grid movement is, therefore, a relative measurement from the camera reference plane.

III. Test Setup

Testing was conducted in Vacuum Facility 11 at the NASA Glenn Research Center. This facility has seven cryogenic pumps with a pumping speed greater than 100,000 L/s with xenon. The facility dimensions are 2.2 m diameter by 7.9 m length. The facility base pressure was approximately 3.0×10^{-5} Pa (2.2×10^{-7} Torr), and the measured pressure at full power was 5.3×10^{-4} Pa (4.0×10^{-6} Torr). The power console and the gas feed system used for this test were similar to that used in Ref. 3.

The thruster and imaging hardware are shown in Fig. 3. The NSTAR thruster, labeled as EMT 3, used during this study was located approximately at the center of the vacuum facility's diameter. This thruster was the same as that used in Ref 3. The neutralizer was a NEXT laboratory model design and is described in Ref. 7. The molybdenum ion optics are engineering model NSTAR optics and are the same design as those used in Ref. 5. The optics are nearly identical in design to those used for spaceflight NSTAR ion thrusters.⁸

The alumina pin, which cannot be resolved in Fig. 3, is mounted at the center of the perforated region of the grids. The long distance camera that monitored the alumina pin and accelerator grid was positioned to the side of the thruster to preclude direct beam ion impingement. The camera and lens were protected from the ion beam plasma and back-sputtered facility material during thruster operation with an aluminum cover. The uncertainty in the measurement was determined to be ± 0.073 mm. Uncertainty analyses include pin thermal expansion, edge detection

and angular camera misalignment. For the steady state values reported in this study, the uncertainty was reduced by averaging the several steady state measurements.

One shortcoming of the measurement technique of Ref. 3 was that the lighting used to illuminate the pin tended to heat the ion optics, causing them to expand by a small amount. Two 500 W halogen bulbs were used to illuminate the titanium ion optics and the alumina pin during the test. For this study, two small white LED spotlights were used to avoid overheating the grids. The spotlights' power loss was 6.8 mW/cm^2 and had a working distance of 100 mm. As shown in Fig. 3, one of the spotlights is located at the bottom of the thruster and the second is also located inside of the aluminum base at the top of the camera. Earlier testing revealed that the best lighting locations were 90° apart from each other.

IV. Test Methodology

The purpose of the test was to measure the transient and steady-state hot grid gaps during thruster operation at different conditions. The test was subdivided in five parts, listed below. Thruster operating conditions during these tests are listed in Table 1.

1. Heating effect of the LED spotlights on the grids – The objective of this test was to determine the effect of grid heating by two LED spotlights. This was done by monitoring the grid gap and grid movement while the spotlights were powered.
2. Startup transient and steady-state operation at low and high power – The purposes of these tests were to measure the transient and steady-state hot grid gaps at the lowest and highest power level of the thruster throttle table. During these tests, the thruster was initially operated without beam extraction until a steady-state hot grid gap was reached. Afterwards, the beam was extracted, and the change in hot grid gap was measured until a steady state value was reached.
3. Steady-state operation at mid-throttle level – The purpose of this test was to measure the steady-state hot grid gap with beam extraction at a middle throttle table power level. During this test, the thruster had been operating at either low or full power and was throttled to TH8. The change in hot grid gap was measured until a steady state value was reached.
4. Transition between power levels – The purpose of these tests was to determine the change in hot grid gap during thruster throttling. The thruster was operated at full power (i.e. TH15) with beam extraction until a steady-state change in hot grid gap was reached. Then, the thruster was throttled down to low power (i.e. TH0). This power level was maintained until a steady-state change in hot grid gap was reached. Finally, the thruster was throttled back to full power.
5. Startup at full power with high voltage applied – During this test, high voltage was applied prior to the ignition of the discharge cathode. As suggested in Ref. 3, this procedure reduces the power deposition, and thus, the heat deposited to the grids. The idea of applying this method is to achieve a reduced change in grid gap during startup.

During some of these tests, ion optics performance parameters that included screen grid ion transparency, electron backstreaming limit, and perveance were measured. The screen grid ion transparency was determined by biasing the screen grid -20 V relative to the discharge cathode potential to repel electrons and monitor the collected ion current. The electron backstreaming limit was determined by lowering the magnitude of the accelerator grid voltage until the indicated beam current increased by 0.1 mA due to backstreaming electrons. Perveance (i.e. the beam current extraction capability of the ion optics) was determined by decreasing the beam voltage and monitoring the accelerator current. Perveance limits were determined from plots of accelerator current as a function of total voltage, where the slope was -0.02 mA/V . Here the total voltage is the sum of the beam power supply voltage and the absolute value of the accelerator grid voltage. Perveance margin is the difference between the nominal total voltage and the total voltage at the perveance limit.

V. Test Results and Discussion

1. Heating Effect of the LED Spotlights

The heating effect of the two LED spotlights is shown in Fig. 4. As the figure shows, the grid gap did not change after about 80 minutes of lighting. The radiant heating from the two LED spotlights was, therefore, not significant enough to affect the grid gap.

2. Startup Transient and Steady-state Grid Gap Change at Low and Full Power

The results for the low power test are plotted in Fig. 5 and 6. The first plot shows the change in hot grid gap as a function of time for low power operation. The neutralizer was ignited first, followed by discharge ignition. The thruster operated without beam extraction until the change in grid gap achieved steady-state. Then, beam extraction was initiated and the thruster operated at the TH0 power level indicated on Table 1. The thruster was turned off at minute 175 and the change in grid gap was monitored for another 40 minutes.

As Fig. 5 shows, operation of the neutralizer caused no change in grid gap. The largest change in grid gap magnitude was reached 15 minutes after discharge ignition and was -0.26 mm. During the low power operation (TH0), the steady-state change in grid gap was -0.17 mm. The grid movement plotted in Fig. 6 suggests that the screen grid thermally expanded more than the accelerator grid.

Figure 7 shows the startup transient and steady-state results for the full power operation. The change in grid gap reached the limit of -0.43 mm imposed by the pin mount screws immediately after discharge ignition. Following discharge ignition, the main and cathode flows were set to their full power levels, even though no beam was extracted. After 107 minutes, the beam was extracted. The steady-state change in grid gap was -0.36 mm.

The thruster was operated on several occasions at low and full power. The steady-state change in grid gap was measured three times at low power and four times at full power. The results are tabulated in Table 2. Average steady-state grid gap changes were -0.20 mm at low power and -0.36 mm at full power.

To ensure that the measured grid gap changes were not somehow adversely affected the test setup, ion optics performance measurements were made and compared to those of Ref. 5. The molybdenum ion optics described in Ref. 5 were the same as those of this study. The resulting electron backstreaming limits, perveance margins, and screen grid ion transparencies are listed in Table 3 along with those of Ref. 5 for comparison. As the table shows, electron backstreaming limits, perveance margins, and screen grid ion transparencies of this investigation were within 1 V, 5 V, and 0.003, respectively, of those measured in Ref. 5. This excellent agreement indicates that the ion optics' hot grid gaps of this study and of Ref. 5 were likely identical.

3. Steady-state Grid Gap Change at Mid-throttle Level

To obtain the steady-state change in grid gap at the mid-throttle level of TH8, the thruster was operated similarly to the aforementioned low power test (Fig 8). The steady-state change in grid gap at the TH8 power level was measured twice and the results are tabulated in Table 2. The average steady-state change in grid gap was -0.36 mm at TH8.

As before, ion optics performance measurements were made and compared to molybdenum ion optics' result of Ref. 5 at this power level. The resulting electron backstreaming limits, perveance margins, and screen grid ion transparencies are listed in Table 3 with those of Ref. 5 for comparison. As the table shows, electron backstreaming limits and perveance margins of this investigation were within 1 V and 5 V, respectively, of those measured in Ref. 5. The screen grid ion transparencies were the same. This excellent agreement indicated that the ion optics' hot grid gaps of this study and of Ref. 5 were likely identical at this power level as well.

4. Transition Grid Gap Change Between Power Levels

To determine the transient grid gap change while transitioning between high and low power, the thruster was operated with beam extraction at full power until a steady-state change in grid gap was achieved, shown in Fig. 9. At minute 187, the thruster was then throttled down to low power. The change in grid gap immediately increased to about -0.11 mm, and then gradually decreased to a steady-state value of -0.20 mm. At minute 276, the thruster was throttled back to full power. The change in grid gap immediately decreased, nearing the limit of -0.43 mm imposed by the pin mount screws. The change in grid gap then increased gradually to the -0.36 mm steady-state value.

These results show that transitioning thruster power from high to low power causes the grid gap change to initially increase before gradually decreasing to a steady-state value. However, transitioning from low to high power rapidly causes the grid gap change to decrease significantly followed by a gradual increase to steady-state grid gap. While transitioning rapidly from high to low power does not appear to present any issues, transitioning rapidly from low to high power could lead to brief periods of electron backstreaming due to the sudden decrease in grid gap. Care must, therefore, be taken to during this transition.

5. Startup at Full Power with High Voltage Applied

Figure 10 shows the results of applying high voltage prior to discharge ignition in an attempt to reduce power deposition to the grids and, therefore, to reduce the differential grid heating effects on the transient hot grid gap. As the figure shows, the change in grid gap reached the limit of -0.43 mm imposed by the pin mount screws immediately after discharge ignition, causing an electrical short between the grids. Therefore, while this technique

will reduce power deposition to the grids, the change in grid gap due to differential grid heating is still significant enough to cause a significant decrease in hot grid gap during startup transients.

6. Comparison of Molybdenum and Titanium Ion Optics Grid Gap Changes

Because the performance of 30 cm titanium ion optics was found to be similar to that of the NSTAR molybdenum ion optics,⁵ the hot grid gaps should also be similar. Furthermore, because both ion optics materials had similar cold grid gaps, the change in grid gaps should also be similar. The steady-state grid gap changes for the titanium optics of Ref. 3 at full and low power were -0.35 mm and -0.19 mm, respectively. These results are nearly identical to those of the molybdenum optics of this study, whose gap changes at full and low power were -0.36 mm and -0.20 mm, respectively. Because grid thicknesses, aperture geometries, cold grid gaps, and grid gap changes were similar for the two optics materials, the performance of the ion optics would also be expected to be similar, and this was demonstrated. This provides additional confirmation that the grid gap measurement technique is determining the molybdenum hot grid gap correctly.

That both ion optics materials exhibited similar hot grid gaps may seem counter-intuitive because titanium has a thermal expansion coefficient that is about 2X that of molybdenum. It is important to note, however, that the hot grid gap is a function of the relative displacements of each grid. Furthermore, the thermal expansion of a grid is not merely a function of its thermal expansion coefficient, but is also a function of its emissivity and thermal conductivity, which will in part set the grid's temperature, and how the grid is mounted, which determines in part how much the grid will expand. Therefore, the hot grid gap is a complex function of several material and mounting system parameters. So, predicting the change in hot grid gap between two ion optics materials by comparing thermal expansion coefficients alone is an incorrect oversimplification.

VII. Conclusions

The change in grid gap of a NSTAR molybdenum ion optics assembly was measured. The measurement technique, similar to that previously applied to a 30 cm titanium ion optics assembly, consisted of measuring the difference in height of an alumina pin, attached to the screen grid, relative to the downstream accelerator grid. The technique was improved with a new illumination system that mitigated grid heating.

Transient and steady-state hot grid gaps were measured at three NSTAR power levels: 0.5, 1.5 and 2.3 kW. The steady-state grid gap changes at these low, middle, and full power levels were measured to be -0.20 mm, -0.36 mm, and -0.36 mm, respectively. Ion optics performance measurements were also made and compared to prior results to ensure that the measured grid gap changes were not adversely affected the test setup. The measured electron backstreaming limits, perveance margins, and screen grid ion transparencies were nearly identical to those of past tests with this ion optics set.

The effect of thruster throttling on the transient grid gap was also measured. While transitioning rapidly from high to low power does not appear to present any issues, transitioning rapidly from low to high power could lead to brief periods of electron backstreaming due to the sudden decrease in grid gap. Care must, therefore, be taken to during this transition.

The hot grid gap changes of molybdenum grids were compared to those of 30 cm titanium ion optics measured in a prior study. Because the cold grid gap, the grid gap changes, the grid thicknesses and aperture geometries were similar for the two optics materials, the performance of the ion optics would also be expected to be similar, and this was demonstrated. This provides additional confirmation of the molybdenum grid gap measurements.

References

- ¹Polk, J.E., et al., "In-Flight Performance of the NSTAR Ion Propulsion System on the Deep Space One Mission," IEEE Aerospace Conference Paper 8.0304, Mar. 2000.
- ²Brophy, J., Marcucci, M., Gates, J., Garner, C., Nakazono, B., and Ganapathi, G., "Status of the Dawn Ion Propulsion System," AIAA-2004-3433, Jul. 2004
- ³Soulas, G.C. and Frandina, M.M., "Ion Engine Grid Gap Measurements," AIAA Paper 2004-3961, Jul. 2004.
- ⁴MacRae, G.S., Zavesky, R.J., and Gooder, S.T., "Structural and Thermal Response of 30 cm Diameter Ion Thruster Optics," AIAA Paper 89-2719, Jul. 1989.
- ⁵Soulas, G.C., "Performance Evaluation of Titanium Ion Optics for the NASA 30 cm Ion Thruster," IEPC Paper 01-92, Oct. 2001.

⁶Soulas, G.C., “Performance of Titanium Optics on a NASA 30 cm Ion Thruster,” AIAA Paper 2000-3814, Jul. 2000.

⁷Soulas, G.C., Domonkos, M.T., and Patterson, M.J., “Performance Evaluation of the NEXT Ion Engine,” AIAA Paper 2003-5278, Jul. 2003.

⁸Christensen, J.A., et al., “Design and Fabrication of a Flight Model 2.3KW Ion Thruster for Deep Space One Mission,” AIAA Paper 1998-3327, July 1998

Table 1. NSTAR thruster operating points.

Power Level Designation	Input Power (KW)	Nominal Beam Current (A)	Beam Voltage (V)	Accelerator Voltage (V)	Main Flow (sccm)	Discharge Cathode Flow (sccm)
TH15	2.3	1.76	1100	-180	23.43	3.7
TH8	1.5	1.10	1100	-180	14.41	2.47
TH0	0.5	0.51	650	-150	5.98	2.47

Table 2. Steady-state change in grid gap at different power levels.

Test	Power Level		
	TH0 (mm)	TH8 (mm)	TH15 (mm)
1	-0.17	N/A	N/A
2	N/A	-0.33	-0.37
3	-0.22	-0.36	-0.36
4	-0.20	N/A	-0.35
5	N/A	N/A	-0.36
Average	-0.20	-0.35	-0.36

Table 3. Ion optics performance comparisons.

Power Level	Electron Backstreaming Limit, V		Perveance Margin, V		Screen Grid Ion Transparency	
	Ref. 5	Present Investigation	Ref. 5	Present Investigation	Ref. 5	Present Investigation
TH0	-69	-68	175	180	0.836	0.834
TH8	-138	-139	455	460	0.877	0.877
TH15	-156	-155	295	300	0.849	0.846



Fig. 1. Upstream side of alumina pin assembly mounted onto the screen grid.

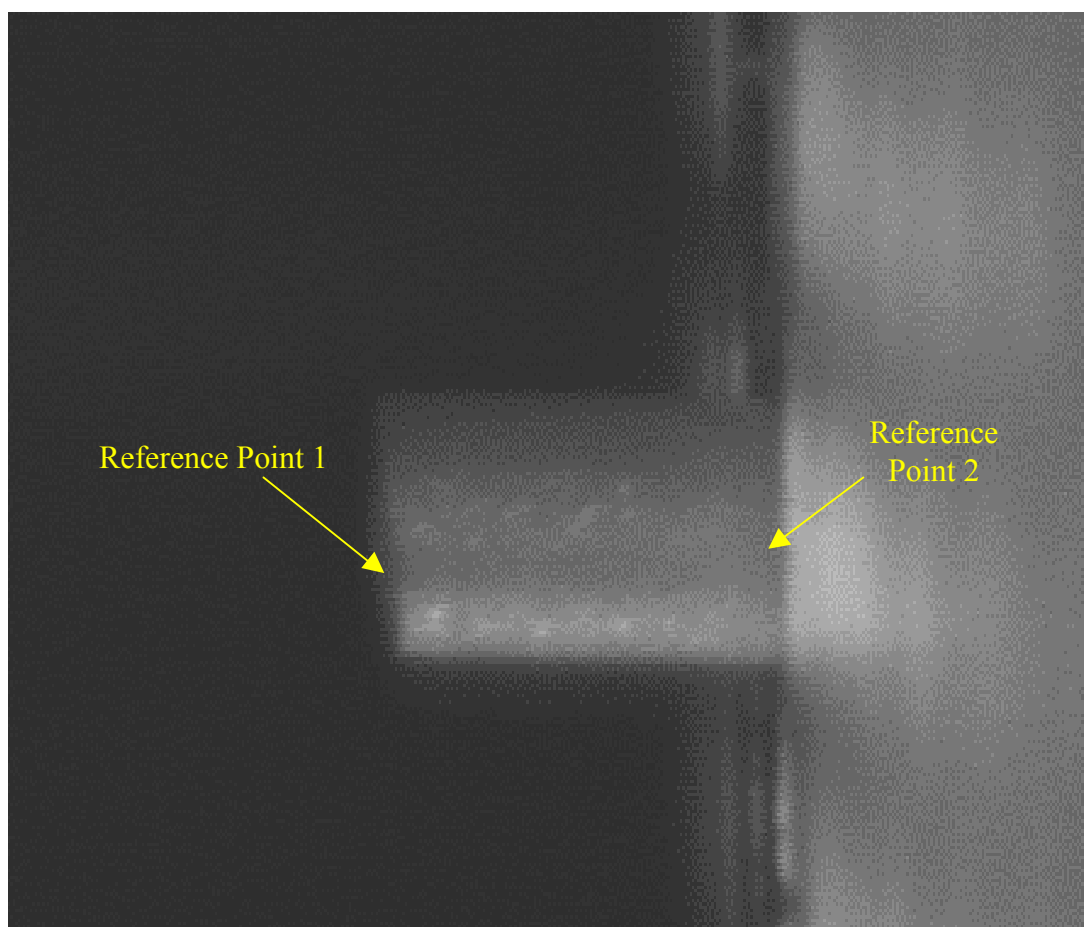


Fig. 2. Sample picture of the alumina pin acquired by the imaging software during thruster operation.

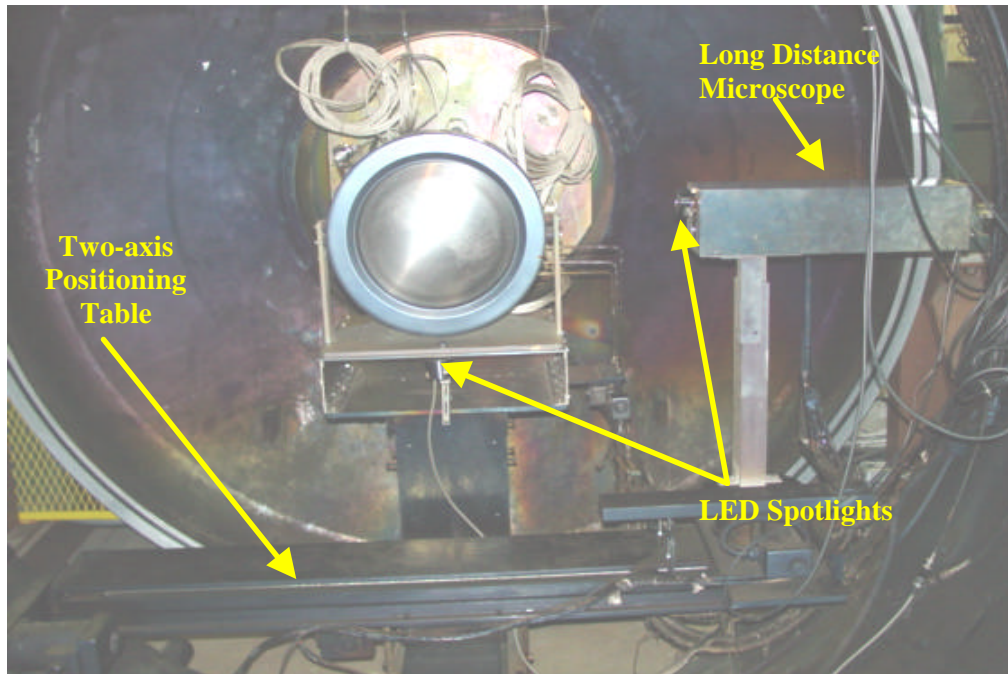


Fig. 3. Test setup.

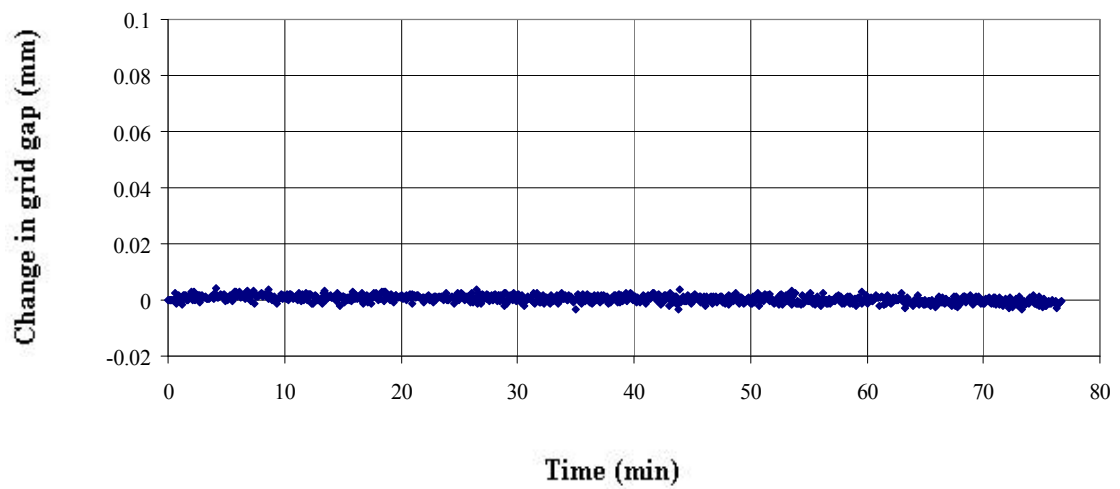


Fig. 3. Change in grid gap as a function of elapsed time due to LED spotlights heating effect.

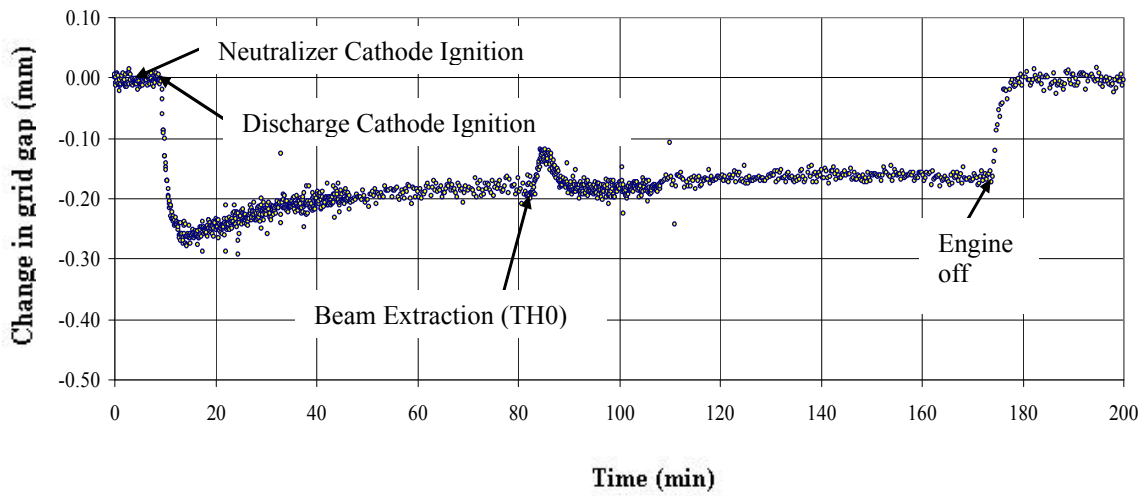


Fig. 4. Change in grid gap as a function of time at low power (i.e. TH0).

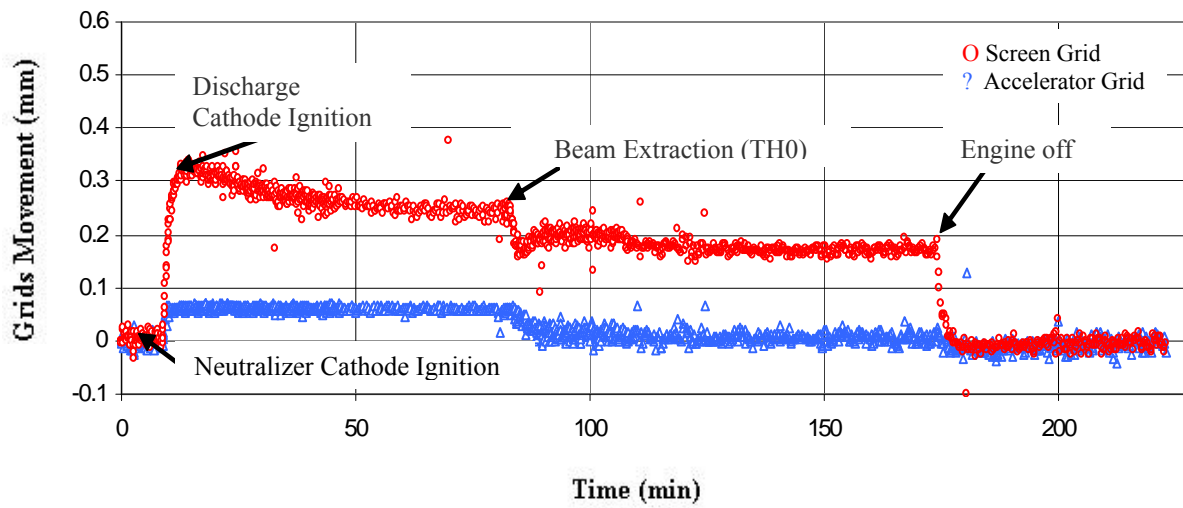


Fig. 5. Grid movement as a function of time at low power (i.e. TH0).

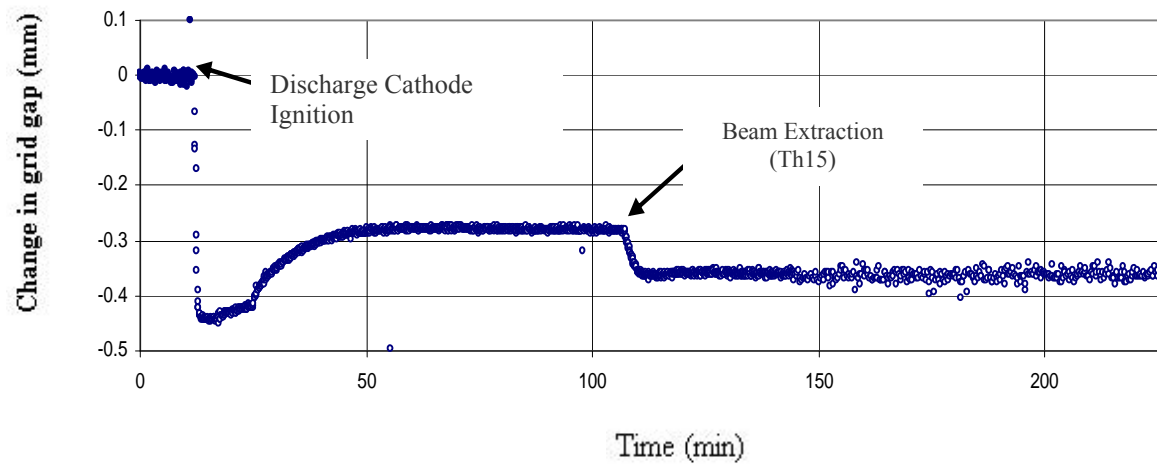


Fig. 6. Change in grid gap as a function of time at full power (i.e. TH15).

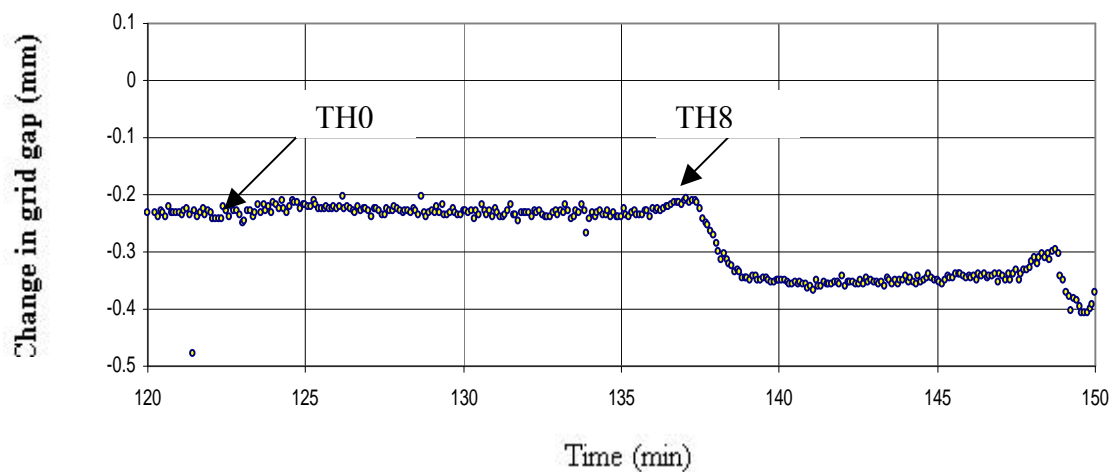


Figure 7. Change in grid gap as a function of time during mid-throttle operation.

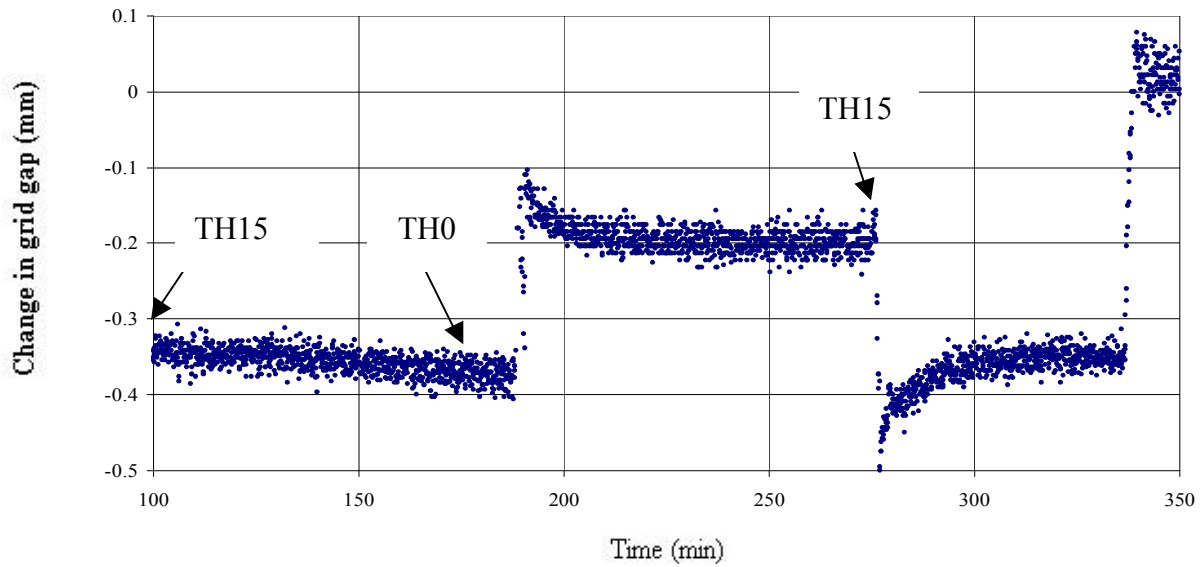


Figure 8. Change in grid gap as a function of time transitioning power levels with beam extraction.

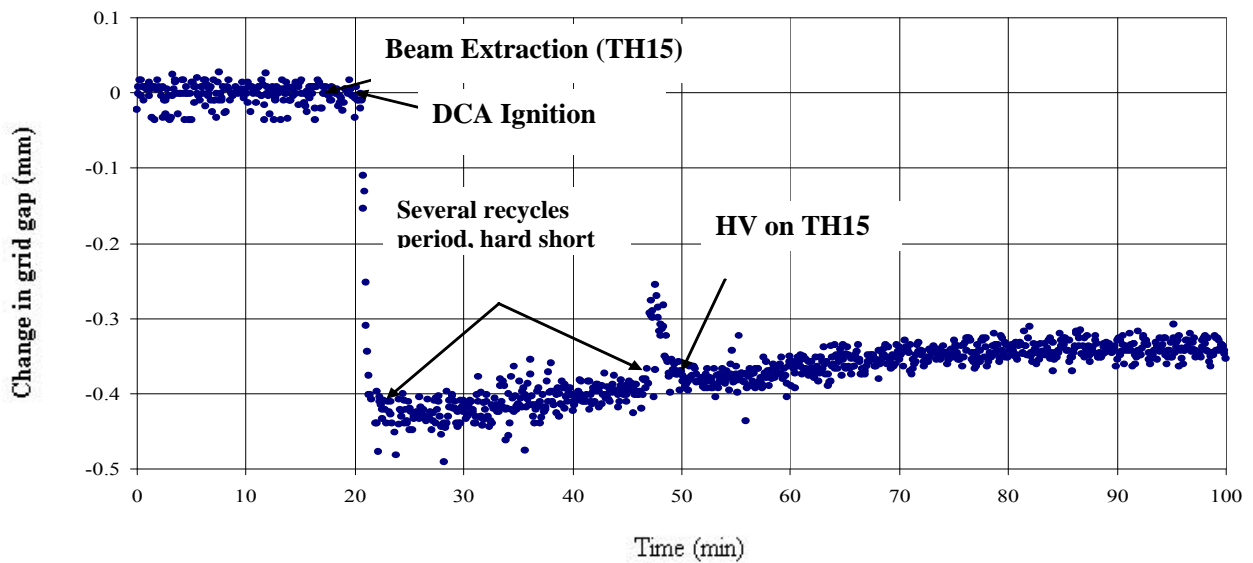


Figure 10. Change in grid gap as a function of time during the startup at full power previous to the discharge ignition.

REPORT DOCUMENTATION PAGE			Form Approved OMB No. 0704-0188	
Public reporting burden for this collection of information is estimated to average 1 hour per response, including the time for reviewing instructions, searching existing data sources, gathering and maintaining the data needed, and completing and reviewing the collection of information. Send comments regarding this burden estimate or any other aspect of this collection of information, including suggestions for reducing this burden, to Washington Headquarters Services, Directorate for Information Operations and Reports, 1215 Jefferson Davis Highway, Suite 1204, Arlington, VA 22202-4302, and to the Office of Management and Budget, Paperwork Reduction Project (0704-0188), Washington, DC 20503.				
1. AGENCY USE ONLY (Leave blank)		2. REPORT DATE April 2006		3. REPORT TYPE AND DATES COVERED Technical Memorandum
4. TITLE AND SUBTITLE Grid Gap Measurement for an NSTAR Ion Thruster			5. FUNDING NUMBERS WBS-22-800-92-71	
6. AUTHOR(S) Esther M. Diaz and George C. Soulas				
7. PERFORMING ORGANIZATION NAME(S) AND ADDRESS(ES) National Aeronautics and Space Administration John H. Glenn Research Center at Lewis Field Cleveland, Ohio 44135-3191			8. PERFORMING ORGANIZATION REPORT NUMBER E-15494	
9. SPONSORING/MONITORING AGENCY NAME(S) AND ADDRESS(ES) National Aeronautics and Space Administration Washington, DC 20546-0001			10. SPONSORING/MONITORING AGENCY REPORT NUMBER NASA TM-2006-214249 IEPC-2005-244	
11. SUPPLEMENTARY NOTES Prepared for the 29th International Electric Propulsion Conference cosponsored by ERPS, Princeton University, NASA Glenn, NASA Jet Propulsion Laboratory, Aerojet, EPPDYL, IEPC, Busek Company, Inc., and Mitsubishi Electric, Princeton, New Jersey, October 31-November 4, 2005. Responsible person, George C. Soulas, organization code RPP, 216-977-7419.				
12a. DISTRIBUTION/AVAILABILITY STATEMENT Unclassified - Unlimited Subject Category: 20 Available electronically at http://gltrs.grc.nasa.gov This publication is available from the NASA Center for AeroSpace Information, 301-621-0390.			12b. DISTRIBUTION CODE	
13. ABSTRACT (Maximum 200 words) The change in gap between the screen and accelerator grids of an engineering model NSTAR ion optics assembly was measured during thruster operation with beam extraction. The molybdenum ion optics assembly was mounted onto an engineering model NSTAR ion thruster. The measurement technique consisted of measuring the difference in height of an alumina pin relative to the downstream accelerator grid surface. The alumina pin was mechanically attached to the center aperture of the screen grid and protruded through the center aperture of the accelerator grid. The change in pin height was monitored using a long distance microscope coupled to a digital imaging system. Transient and steady-state hot grid gaps were measured at three power levels: 0.5, 1.5 and 2.3 kW. Also, the change in grid gap was measured during the transition between power levels, and during the startup with high voltage applied just prior to discharge ignition. Performance measurements, such as perveance, electron backstreaming limit and screen grid ion transparency, were also made to confirm that this ion optics assembly performed similarly to past testing. Results are compared to a prior test of 30 cm titanium ion optics.				
14. SUBJECT TERMS Propulsion; Electric propulsion; Electrostatic propulsion; Ion propulsion			15. NUMBER OF PAGES 17	
			16. PRICE CODE	
17. SECURITY CLASSIFICATION OF REPORT Unclassified	18. SECURITY CLASSIFICATION OF THIS PAGE Unclassified	19. SECURITY CLASSIFICATION OF ABSTRACT Unclassified	20. LIMITATION OF ABSTRACT	

